ESC European Society of Cardiology

European Heart Journal - Cardiovascular Imaging (2024) **25**, 285–292
https://doi.org/10.1093/ehjci/jead246

ORIGINAL PAPER

Incremental prognostic value of downstream positron emission tomography perfusion imaging after coronary computed tomography angiography: a study using machine learning

Eero Lehtonen [1†], Iida Kujala [1†], Jonne Tamminen[1], Teemu Maaniitty [1,2], Antti Saraste [1,3], Jarmo Teuho [1], Juhani Knuuti [1,2], and Riku Klén [1*]

[1]Turku PET Centre, Turku University Hospital and University of Turku, Turku, Finland; [2]Department of Clinical Physiology, Nuclear Medicine and PET, Turku University Hospital, Turku, Finland; and [3]Heart Center, Turku University Hospital and University of Turku, Turku, Finland

Received 30 June 2023; revised 7 September 2023; accepted 22 September 2023; online publish-ahead-of-print 29 September 2023

Aims To evaluate the incremental value of positron emission tomography (PET) myocardial perfusion imaging (MPI) over coronary computed tomography angiography (CCTA) in predicting short- and long-term outcome using machine learning (ML) approaches.

Methods and results A total of 2411 patients with clinically suspected coronary artery disease (CAD) underwent CCTA, out of whom 891 patients were admitted to downstream PET MPI for haemodynamic evaluation of obstructive coronary stenosis. Two sets of Extreme Gradient Boosting (XGBoost) ML models were trained, one with all the clinical and imaging variables (including PET) and the other with only clinical and CCTA-based variables. Difference in the performance of the two sets was analysed by means of area under the receiver operating characteristic curve (AUC). After the removal of incomplete data entries, 2284 patients remained for further analysis. During the 8-year follow-up, 210 adverse events occurred including 59 myocardial infarctions, 35 unstable angina pectoris, and 116 deaths. The PET MPI data improved the outcome prediction over CCTA during the first 4 years of the observation time and the highest AUC was at the observation time of Year 1 (0.82, 95% confidence interval 0.804–0.827). After that, there was no significant incremental prognostic value by PET MPI.

Conclusion PET MPI variables improve the prediction of adverse events beyond CCTA imaging alone for the first 4 years of follow-up. This illustrates the complementary nature of anatomic and functional information in predicting the outcome of patients with suspected CAD.

* Corresponding author. E-mail: riku.klen@utu.fi
† These authors contributed equally to this work.

Graphical Abstract

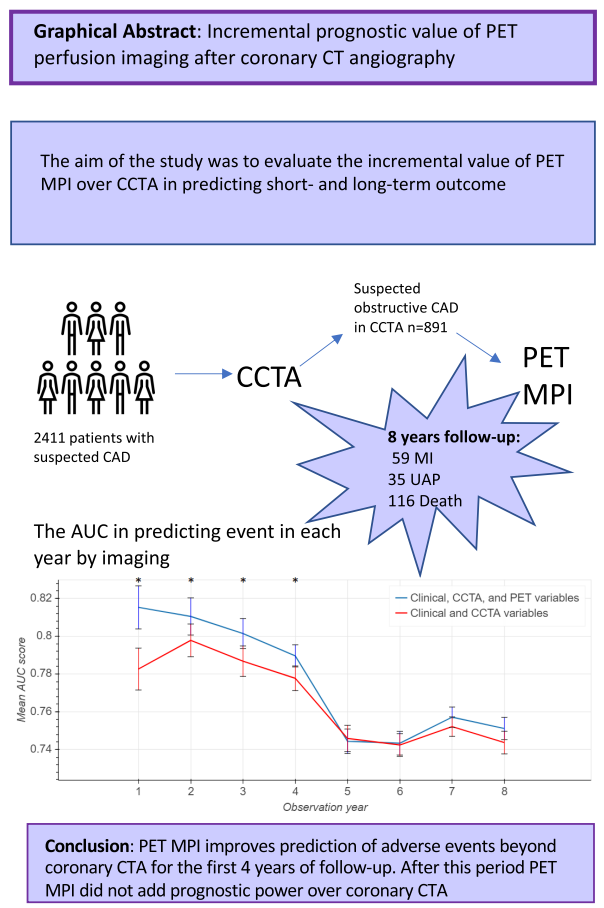

Keywords positron emission tomography • myocardial perfusion imaging • coronary computed tomography angiography • machine learning • extreme gradient boosting

Introduction

Coronary artery disease (CAD) is a leading cause of death globally. Coronary computed tomography angiography (CCTA) is an accurate non-invasive imaging method to diagnose or exclude coronary atherosclerosis and obstructive CAD.[1] CCTA gives information on the extent of atherosclerotic findings, their distribution, and severity. On the other hand, myocardial perfusion imaging (MPI) enables the detection of functionally significant coronary artery stenoses and myocardial ischaemia. In hybrid imaging, CCTA and MPI are combined to accurately assess anatomical changes as well as ischaemia, both at the patient level and regionally from each coronary artery.[2]

Hybrid imaging may be useful for identification of patients who are at high risk of developing acute coronary syndrome (ACS). In patients with intermediate coronary lesions, evidence of ischaemia at an anatomically appropriate location by hybrid imaging is associated with an increased rate of subsequent death or cardiac adverse events.[3–5] Although the complementary nature of the anatomical and functional imaging is well established, there is only limited evidence of how each method can predict events in the short and the long term. We hypothesize that ischaemia as a sign of more severe CAD is stronger in predicting short-term outcome while anatomical findings, reflecting also earlier phases of the development of CAD, may be better in predicting adverse events in the long term.

Previous studies suggest that machine learning (ML) is feasible and can improve the risk stratification of patients with suspected or established CAD.[6,7] Previous studies have shown that the risk of the cardiac event is determined by both clinical risk factors and imaging-derived findings.[8] Combining both CCTA and clinical risk factors into ML models seems to predict all-cause mortality significantly better than either alone.[9] Recently, an XGBoost ML model trained on clinical data, CT quantitative plaque measures, and ^{18}F-NaF uptake was used for optimized risk stratification in patients with CAD.[8] Substantial improvement over traditional methods for risk stratification was achieved when all available factors (clinical and imaging) were included in the ML model.

The goal of the presented work was to evaluate the incremental value of positron emission tomography (PET) MPI over CCTA in predicting major adverse events. To achieve this, ML was used as a tool to assess the predictive power of CCTA and PET MPI both in the short and long term.

Methods

Cohort

We retrospectively collected data from symptomatic (chest pain and/or dyspnoea) patients who have undergone selective hybrid PET/CCTA in

Turku PET Centre due to clinically suspected CAD between February 2007 and December 2016. Patients with prior known CAD were not included. Our cohort consists of a total of 2411 patients. Out of these, 864 patients have been previously reported in Maaniitty *et al.*,[10] 670 patients in Stenström *et al.*,[11] 530 patients in Harjulahti *et al.*,[12] and 830 patients in Benjamins *et al.*[13] The novelty of the present manuscript is the application of ML methods as well as the inclusion of more patients and longer follow-up time.

After removal of incomplete data entries, data from 2284 patients (42% male) were retained for further analysis. Following our clinical routine, patients first undergo CCTA using a hybrid PET–CT scanner, and immediately after that, the attending physician performs an initial evaluation of the CCTA scan. If obstructive CAD is excluded by CCTA, no further imaging procedures are performed. In case of the presence of obstructive CAD (diameter stenosis ≥50%) or if obstructive CAD cannot be excluded by CCTA, PET MPI is performed.

Data collection and follow-up

Imaging results, symptoms, and cardiovascular risk factors were retrospectively collected from electronic medical records and saved to the database by investigators. CCTA and perfusion imaging results were obtained from the institutional imaging database. Primary endpoints of follow-up data included all-cause death, myocardial infarction (MI), and unstable angina pectoris (UAP). Comprehensive data on the occurrence of all-cause death, MI, and UAP until May 2020 were obtained from the registries of the Finnish Institute for Health and Welfare and the Centre for Clinical Informatics of the Turku University Hospital. Investigators used electronic medical records to validate all adverse events. If an event occurred, the time difference in years between the CCTA scan and the event was recorded. The observation time is the time interval starting from the CCTA scan until the date of the first occurrence of an event or the end date of follow-up (13 May 2020), whichever happened first. In the analyses with limited observation time, we considered only the events that took place within the limited time. Data on early revascularization (≤6 months), with either percutaneous coronary intervention (PCI) or coronary artery bypass graft surgery (CABG), were collected but were not used as endpoints.

Imaging methods and metrics

The CCTA and PET MPI imaging methods have been previously described.[10,14] CCTA scans were performed using a 64-row hybrid PET–CT scanner (GE Discovery VCT or GE D690, General Electric Medical Systems, Waukesha, WI, USA). Collimation was set at 64 × 0.625 mm, gantry rotation time was 350 ms, tube current 500–750 mA, and voltage 100–1x20 kV, depending on patient size. Before CCTA, beta-blocker (metoprolol, 0–30 mg) was given intravenously to achieve a target heart rate of <60 beats/min. Isosorbide dinitrate aerosol (1.25 mg) was administered to achieve coronary dilation. CCTA was performed using intravenously administered low-osmolal iodine contrast agent followed by saline flush. Prospectively triggered acquisition was applied whenever feasible. From CCTA, we determined the severity of stenosis for each segment of the main coronary arteries (LM, LAD, LCX, RCA) and side branches (D1, D2, LOM1, LOM2, LDP, LPL, RPD, RPL, IM). The presence, extent, and severity of coronary atherosclerosis were evaluated by defining the number of coronary artery segments with any atherosclerosis (also known as segment involvement score), the number of segments with non-obstructive (<50%) plaque, and the number of segments with obstructive (≥50%) plaque (details in Supplementary data online).

Based on the CCTA findings, patients with suspected obstructive CAD (≥50% diameter stenosis in ≥1 coronary artery segment) underwent PET MPI with ^{15}O–water during adenosine stress, as previously described.[10,14] The tracer was injected as an intravenous bolus (mean injected activity 900–1100 MBq) over 15 s, and dynamic PET acquisition was performed (14 × 5, 3 × 10, 3 × 20, and 4 × 30 s). Absolute stress myocardial blood flow (asMBF) was quantified (in mL/g/min) individually for each of the 17 myocardial segments separately, excluding basal septal segments due to membranous part (standard Segments 2 and 3). Myocardial perfusion ≥ 2.3 mL/g/min is considered as normal.[15] Rest myocardial blood flow was not included in analysis as rest perfusion imaging is not routinely performed in our institution (stress-only protocol).[16] We define the stress myocardial blood flow (sMBF) abnormality score as

$$\mathrm{sMBF} = \max(0, 2.3 - \mathrm{asMBF}),$$

so that the zero score corresponds to normal flow. Zero imputation was applied for the sMBF scores for patients who did not undergo PET MPI (or for whom the PET MPI failed) for the whole study cohort.

Clinical data

Data on traditional risk factors [smoking, sex, body mass index (BMI), diabetes mellitus, hypertension, dyslipidaemia, and family history of CAD] were collected from electronic medical records. Symptoms were classified as either typical angina pectoris, atypical (atypical angina pectoris or non-anginal chest pain), or no chest pain. Also, a history of dyspnoea was collected. A summary of the clinical data is presented in *Table 1* in Results.

Machine learning, XGBoost

ML models were trained and used to predict major adverse events by incorporating clinical cardiovascular risk factors and CCTA and PET imaging data. For the training of each model, data were split randomly and independently into training and test groups with a 3:1 ratio. Each variable was checked individually to ensure similar distributions in both groups as described in the Supplementary data online.

For this study, we considered several models, including linear regression, lasso,[17] support vector machine,[18] ridge,[19] elastic net,[20] logistic regression,[21] random forest,[22] and Extreme Gradient Boosting,[23] also known as XGBoost. Of these, XGBoost consistently performed the best in the preliminary analysis and was selected as the ML method to generate the results of this paper.

To simplify the XGBoost models presented in Results, we computed feature importance vectors for 100 XGBoost models trained with all considered input variables—in total 53 variables containing 20 PET-based variables—for each observation year 1–8 and selected nine input variables which were ranked consistently as the most important features. An independent random training and test data split, as described in the Supplementary data online, was performed for each of the 100 XGBoost models. Supplementary data online, *Table S1* presents the feature ranking vector used for the selection of variables of the XGBoost models. These selected nine input variables in the descending order of importance are maximum stenosis degree (a CCTA-based variable), number of atherosclerotic segments (CCTA), number of non-obstructive segments (CCTA), age, maximum PET abnormality score for RCA (a PET-based variable), BMI, sMBF for Segment 10 (PET), sMBF for Segment 15 (PET), and dyspnoea. We define the maximum PET abnormality score for RCA as:

$$s_{\mathrm{maxRCA}} = \text{maximum sMBF across segments 4, 9, 10 and 15.}$$

The preprocessing of variables is described in detail in the Supplementary data online, as are the hyperparameter selection for the considered XGBoost model, and the training and test set division. For the results presented in this work, we trained two sets of XGBoost models for each observation year: the first set uses clinical, CCTA-based, and PET-based input variables, while the other set uses only clinical and CCTA-based variables. Per each observation year, each set consists of $k = 100$ XGBoost models, each trained and tested using an independent and random training and test data split. Furthermore, we considered 2 sets of data for the analyses: the data set corresponding to all considered 2284 patients, and its subset of 2069 patients who did not undergo early revascularization, as explained in more detail in Results. For the set of all considered 2284 patients, each

Table 1 Demographics table

	All patients ($n = 2284$)	Patients with no early revascularization ($n = 2069$)
Age (years)	(23.0–88.0), 62.2 ± 9.7	(23.0–88.0), 62.0 ± 9.8
Women	1317 (57.7%)	1249 (60.4%)
BMI	(15.4–54.3), 28.3 ± 5.2	(15.4–54.3), 28.3 ± 5.2
Smoking	757 (33.1%)	657 (31.8%)
Diabetes	341 (14.9%)	289 (14.0%)
Hypertension	1292 (56.6%)	1155 (55.8%)
Dyslipidaemia	1456 (63.7%)	1287 (62.2%)
Dyspnoea	877 (38.4%)	791 (38.2%)
Atypical angina or non-anginal chest pain	1083 (47.4%)	1004 (48.5%)
Typical angina	528 (23.1%)	432 (20.9%)
CCTA and PET findings		
Normal coronary arteries	718 (31.4%)	718 (34.7%)
Non-obstructive CAD	636 (27.8%)	636 (30.7%)
Obstructive CAD and normal sMBF	403 (17.6%)	392 (18.9%)
Obstructive CAD and abnormal sMBF	400 (17.5%)	233 (11.3%)
Endpoints	210 (9.2%)	172 (8.3%)
MI	59 (2.6%) (28.1% of all endpoints)	46 (2.2%) (26.7% of all endpoints)
UAP	35 (1.5%) (16.7% of all endpoints)	19 (0.9%) (11.0% of all endpoints)
Death	116 (5.1%) (55.2% of all endpoints)	107 (5.2%) (62.2% of all endpoints)
Early revascularization		
PCI	180 (7.9%)	0 (0%)
CABG	40 (1.8%)	0 (0%)

Clinical characteristics, imaging findings, endpoints, and early invasive therapies of all patients and patients with no early revascularization separately.
CAD, coronary artery disease; CABG, coronary artery bypass grafting; CCTA, coronary computed tomography angiography; MI, myocardial infarction; PCI, percutaneous coronary intervention; PET, positron emission tomography; sMBF, stress myocardial blood flow; UAP, unstable angina pectoris.

training set contains 1713 patients (75%) and each test set contains 571 patients (25%). The same XGBoost models—and hence training and test sets—were used for analysing the results corresponding to all the 2284 patients and corresponding to the subset of 2069 patients by restricting the result analysis to only those patients who did not undergo revascularization. A flow diagram of this work is illustrated in *Figure 1*.

Statistical analyses

Statistically significant differences between the areas under the receiver operator characteristic curves (AUCs) corresponding to all data variables and data without PET variables were assessed using the two-sided Wilcoxon signed-rank test with $P = 0.05$. The representation of variables is described in the Supplementary data online in the Preprocessing subsection.

Results

The study cohort consisted of 2284 patients who underwent CCTA due to suspected CAD, of whom 891 (39%) underwent downstream PET MPI for evaluation of haemodynamic significance of coronary stenosis. As shown in *Table 1*, 31.4% of patients had normal coronary arteries, 27.8% had non-obstructive CAD, 17.6% had obstructive CAD on CCTA but normal myocardial perfusion on PET, and 17.5% had obstructive CAD and abnormal myocardial perfusion. The remaining 5.7% of the patients consist of those who did not undergo PET MPI despite suspected CAD, and of those whose PET perfusion imaging study was unsuccessful or whose PET MPI data were missing. The clinical characteristics of patients are presented in *Table 1*.

During the 8-year follow-up period, 210 patients had major adverse event (Year 1: 33 events, Year 2: 18 events, Year 3: 30 events, Year 4: 28 events, Year 5: 31 events, Year 6: 32 events, Year 7: 21 events, Year 8: 17 events). Of these endpoints, 28.1% correspond to MI, 16.7% to UAP, and 55.2% to death. In total, 215 patients had early revascularization within 6 months after CCTA, with percutaneous coronary intervention (PCI) ($n = 180$), coronary artery bypass graft (CABG) surgery ($n = 40$), or both ($n = 5$). Of note, early revascularization was not considered as a major adverse event.

Figure 2 shows the results of the XGBoost ML models in predicting outcome (event or no event) for each observation time (1–8 years) using the random and independent test sets ($N = 571$). In *Figure 1*, AUCs and their 95% confidence intervals (CIs) are visualized for the two sets of Xboost models: (i) with all input variables and (ii) without PET variables.

The results show that the predictive power of the data is reducing over time from the best AUC of 0.82 (95% CI 0.804–0.827) at Year 1 of the observation time to AUC of 0.75 (95% CI 0.745–0.757) at the maximum observation time of 8 years. The AUCs with the data including PET variables were significantly higher than when using only clinical and CCTA variables ($P < 0.05$). However, the significant difference was detected only during the first 4 years of the observation time.

As revascularization is used to treat ischaemia and is strongly linked with the ischaemic imaging findings,[11] we performed a separate analysis

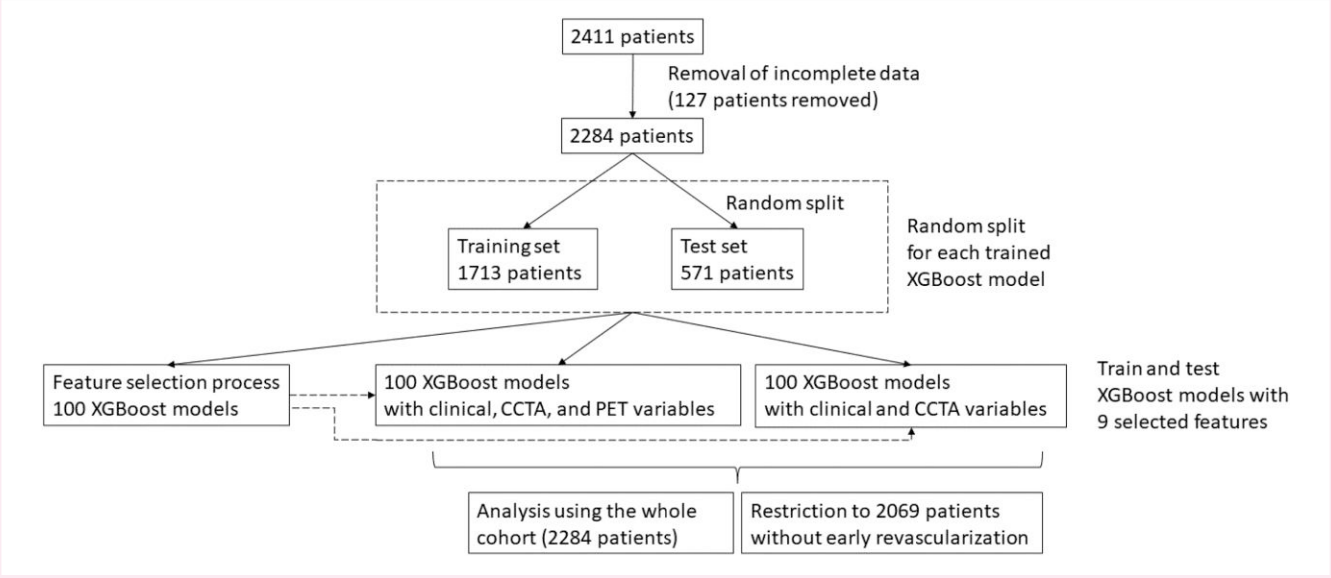

Figure 1 Flow diagram of the presented work. After removal of incomplete data entries, data from 2284 patients were retained for further analysis. In the feature selection process, 100 XGBoost models were trained using all the considered input variables, and based on the testing of these models, 9 most important features were selected. These nine variables were considered in training and testing of two sets of 100 XGBoost models (using clinical, CCTA, and PET variables vs. using only clinical and CCTA variables). Finally, we considered the subsets of the test data, restricted to patients who did not undergo early revascularization.

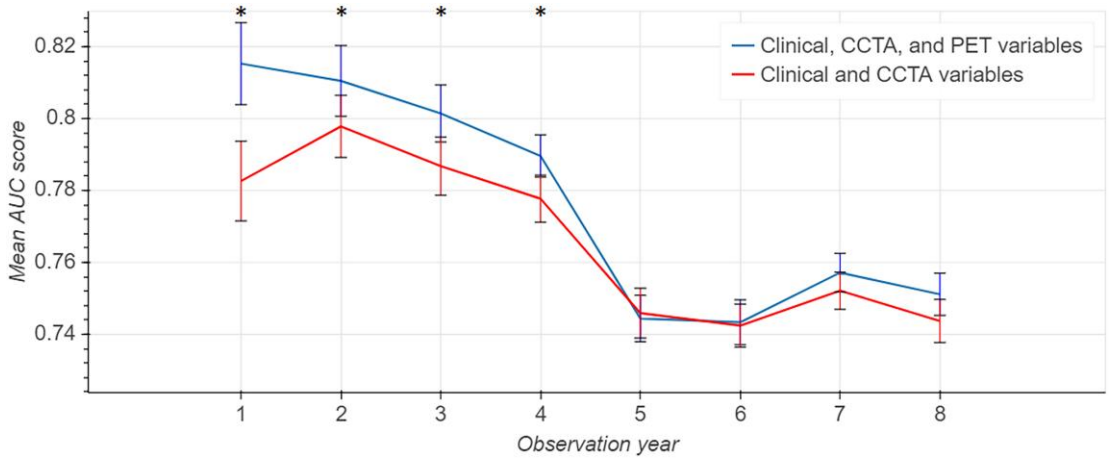

Figure 2 Mean AUCs and 95% CIs for the XGBoost models trained with all variables, and without PET variables in the test sets randomly selected from the whole cohort. Per each observation year, 100 XGBoost models were trained and tested for each input variable set; an independent and random training and test data split was performed for each of these models. The AUCs are calculated using the test sets ($N = 571$). The difference between these curves is statistically significant for the first four observation years; this is highlighted by the black asterisks.

restricted to patients without early revascularization, as illustrated in *Figure 3*. In this analysis, there was no statistically significant difference between the mean AUCs.

Figure 4 illustrates the mean AUC difference curves for XGBoost models trained with all the variables and without PET variables, separately drawn for all patients and patients without early revascularization. The difference between the curves is larger during the first 4 years of observation time and becomes diminished with time.

Discussion

Predicting the outcome of patients with suspected CAD is one of the main goals of diagnostic testing. The imaging methods used for the diagnosis of CAD are well known to also provide prognostic information. Furthermore, combining data from anatomical imaging and functional imaging may further improve the predictive power.[10] We use ML in predicting outcome, as it enables the automated fusion of large number

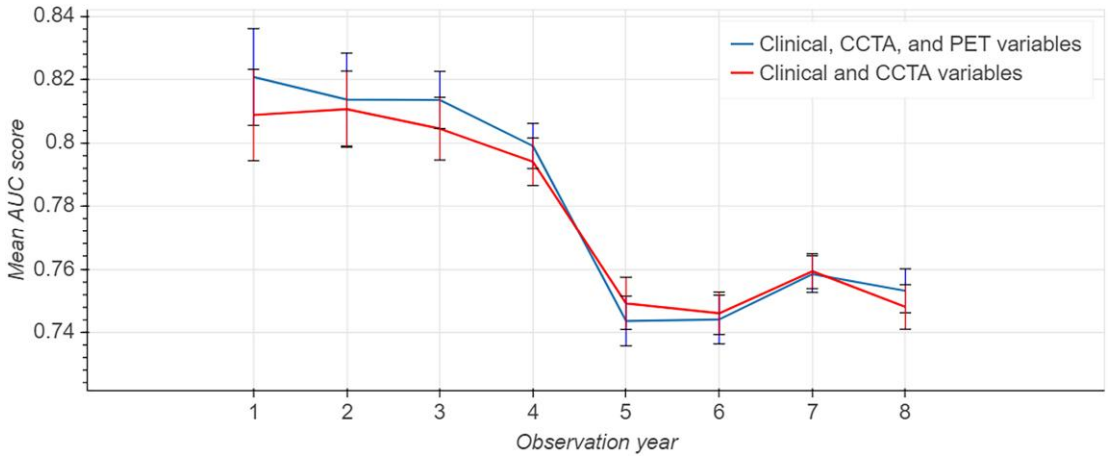

Figure 3 Mean AUCs and 95% CIs for the restricted set of patients who did not undergo early revascularization. The XGBoost models trained with all variables, and without PET variables using the whole cohort data. The AUCs are calculated using the same test sets as in the whole cohort case, restricted to patients who did not undergo early revascularization.

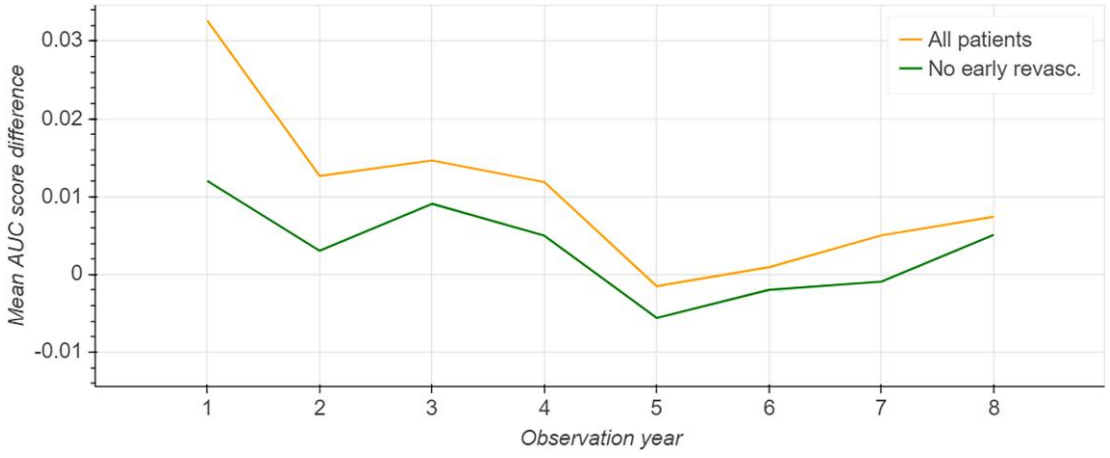

Figure 4 Mean AUC differences (all variables vs. no PET variables) for XGBoost models trained and tested with data corresponding to all patients, and with data corresponding to patients without early revascularization.

of input variables—our analysis began with 53 different input variables. In particular, the chosen ML framework, XGBoost, has been applied previously with state-of-the-art results to various ML and data mining challenges.[23] The highest AUC in the presented study for predicting event was 0.82 which is comparable to the highest score reported in an earlier study combining atherosclerotic plaque microcalcification and anatomical features of CAD (0.85, 95% CI 0.79–0.91).[8]

Our findings support the hypothesis that the presence of ischaemia as a sign of more severe CAD could be stronger in predicting short-term outcome while anatomical findings, reflecting also earlier phases of the development of CAD, might be better in predicting events in the long term. The predictive power increased by adding myocardial perfusion parameters on top of the clinical and CCTA variables, but this impact was only seen during the first 4 years.

In contrast to our study, in a recent study utilizing SPECT/CCTA, hybrid imaging provided independent prognostic information for short- and long-term risk prediction.[24,25] Unlike in our work, the prognostic benefit of hybrid imaging lasted for 10 years (median 6.8) follow-up.[24] However, in that study, the patient population was rather small (n = 357) and included only 46 patients with matched anatomical stenosis and perfusion deficit.[24]

The incremental prognostic value of perfusion imaging was not detected when the patients with early revascularization were excluded (note that early revascularization was not used as an endpoint). We have earlier shown, in partly overlapping patient population, that the adherence of early revascularization to myocardial ischaemia detected by PET perfusion imaging is very high.[11] As the ischaemic finding triggers revascularization, a large proportion of the high-risk patients based on the perfusion findings did enter the revascularization procedure and were, therefore, excluded from the secondary analysis. These findings further suggest that the increased event risk is associated with abnormal perfusion, which commonly triggers revascularization procedures to eliminate ischaemia. This is consistent with previous studies showing an interplay between the severity of ischaemia, myocardial

revascularization, and outcomes.[26–29] However, our study emphasizes that the residual risk of an event is still significant despite revascularization. This risk is likely associated with generally more severe CAD in the patients with detected ischaemia in the diagnostic phase.

In the clinical routine protocol applied in our hospital, the downstream PET perfusion imaging is triggered by abnormal CCTA finding, as suggested by the current European guidelines.[30] This approach is based on the high negative predictive value of CCTA in excluding obstructive CAD and excellent outcome of patients without obstructive CAD, obviating the need for further diagnostic testing in over half of symptomatic patients with suspected CAD.[10,31] Due to this, the patients who entered perfusion imaging were selected based on CCTA findings, and therefore, our results can be only transferred to similar situations than in the present study.

As limitations of the current work, we note that it is a single-centre study, and the numbers of events in test data sets are unavoidably quite small (in the whole data set, there are 17–33 events per year). Furthermore, the treatment of patients is not blinded and can affect the results. It should be noted that our ML model included all patients referred to CCTA regardless of the performance of downstream PET perfusion imaging. For patients with obstructive CAD excluded by CCTA alone, and therefore not undergoing further PET imaging, were classified as having non-obstructive CAD. We think that this method resembles the clinical setting in which a patient has obstructive CAD excluded by CCTA and no further testing is performed, although we acknowledge that, for example, coronary microvascular dysfunction can impair myocardial blood flow in the absence of obstructive epicardial CAD. Another potential limitation is that we did not measure detailed CCTA characteristics for prognostic information, such as quantitative plaque volumes, but, on the other hand, the CCTA variables in our study are those that are widely used in clinical practice.[32] We used 64-row CT scanners that are fulfilling the current requirements for CCTA but believe that the results should be generalizable also to CCTA scanners with a higher number of rows because the scans were analysed by experienced human readers and these features were subsequently provided as an input for the ML algorithm rather than directly feeding the CCTA images for the model. Furthermore, we could not include PET rest myocardial blood flow values into this study, as the considered study used stress-only protocol.[16] However, according to a previous study from our institution,[16] absolute stress MBF was superior to perfusion reserve (i.e. stress MBF divided by rest MBF) in the detection of haemodynamically significant CAD.

Interestingly, ML determined some specific regional PET perfusion results as selected features, mostly located to the inferior wall of the left ventricle and area supplied by RCA. This selection by the XGBoost model is difficult to understand as classically anterior ischaemia has been considered prognostically the most important.

Conclusion

Based on the ML approach, downstream MPI after CCTA improves the prediction of adverse events beyond CCTA alone for the 4 years of follow-up, but no longer-term benefit was seen. The results illustrate the differences and complementary nature of anatomic and functional information in predicting the outcome of patients with chest pain and suspected CAD.

Supplementary data

Supplementary data are available at *European Heart Journal - Cardiovascular Imaging* online.

Funding

Authors acknowledge financial support by grants from the Academy of Finland, the Finnish Foundation for Cardiovascular Research, the Finnish Cultural Foundation, and the State Research Funding of Turku University Hospital.

Conflict of interest: J.K. received consultancy fees from GE Healthcare and AstraZeneca and speaker fees from GE Healthcare, Bayer, Lundbeck, Boehringer-Ingelheim, Pfizer, and Merck, outside of the submitted work. A.S. received consultancy fees from Amgen and Astra Zeneca, Boehringer-Ingelheim, and Pfizer, and speaker fees from Abbott, Astra Zeneca, and Bayer. All other authors have reported that they have no relationships relevant to the contents of this paper to disclose.

Data availability

The data underlying this article cannot be shared publicly due to the privacy of individuals that participated in the study. The data will be shared on reasonable request to the corresponding author.

Author contributions

All authors contributed to the study conception and design. Material preparation, data collection, and analysis were performed mainly by E.L., I.K., T.M., and J.T. The first draft of the manuscript was written by E. L., I.K., T.M., J.T., R.K., and J.K., and all authors commented on previous versions of the manuscript. All authors read and approved the final manuscript. The first two authors contributed equally: E.L. oversaw the algorithm development and mathematical part of this work, while I.K. was in charge of the medical part of this work, and both of the first authors equally contributed to the writing of the manuscript.

Ethics approval

The study complies with the Declaration of Helsinki. The Ethics Committee of the Hospital District of Southwest Finland approved the study protocol and waived the need for written informed consent by patients due to observational nature.

References

1. Budoff MJ, Dowe D, Jollis JG, Gitter M, Sutherland J, Halamert E *et al.* Diagnostic performance of 64-multidetector row coronary computed tomographic angiography for evaluation of coronary artery stenosis in individuals without known coronary artery disease: results from the prospective multicenter ACCURACY (Assessment by Coronary Computed Tomographic Angiography of Individuals Undergoing Invasive Coronary Angiography) trial. *J Am Coll Cardiol* 2008;**52**:1724–32.
2. Danad I, Raijmakers PG, Driessen RS, Leipsic J, Raju R, Naoum C *et al.* Comparison of coronary CT angiography, SPECT, PET, and hybrid imaging for diagnosis of ischemic heart disease determined by fractional flow reserve. *JAMA Cardiol* 2017;**2**:1100–7.
3. Hadamitzky M, Achenbach S, Al-Mallah M, Berman D, Budoff M, Cademartiri F *et al.* Optimized prognostic score for coronary computed tomographic angiography: results from the CONFIRM registry (COronary CT Angiography EvaluatioN For Clinical Outcomes: An InteRnational Multicenter registry). *J Am Coll Cardiol* 2013;**62**:468–76.
4. Hadamitzky M, Freißmuth B, Meyer T, Hein F, Kastrati A, Martinoff S *et al.* Prognostic value of coronary computed tomographic angiography for prediction of cardiac events in patients with suspected coronary artery disease. *JACC Cardiovasc Imaging* 2009;**2**:404–11.
5. Chow BJ, Small G, Yam Y, Chen L, Achenbach S, Al-Mallah M *et al.* Incremental prognostic value of cardiac CT in CAD using CONFIRM (COroNary computed tomography angiography evaluation for clinical outcomes: an InteRnational Multicenter registry). *Circ Cardiovasc Imaging* 2011;**4**:463–72.
6. Juarez-Orozco LE, Martinez-Manzanera O, van der Zant FM, Knol RJJ, Knuuti J. Deep learning in quantitative PET myocardial perfusion imaging: a study on cardiovascular event prediction. *JACC Cardiovasc Imaging* 2020;**13**:180–2.
7. Haro Alonso D, Wernick MN, Yang Y, Germano G, Berman DS, Slomka P. Prediction of cardiac death after adenosine myocardial perfusion SPECT based on machine learning. *J Nucl Cardiol* 2019;**26**:1746–54.
8. Kwiecinski J, Tzolos E, Meah MN, Cadet S, Adamson PD, Grodecki K *et al.* Machine learning with 18F-sodium fluoride PET and quantitative plaque analysis on CT angiography for the future risk of myocardial infarction. *J Nucl Med* 2022;**63**:158–65.

9. Motwani M, Dey D, Berman DS, Germano G, Achenbach S, Al-Mallah MH *et al.* Machine learning for prediction of all-cause mortality in patients with suspected coronary artery disease: a 5-year multicentre prospective registry analysis. *Eur Heart J* 2017;**38**:500–7.
10. Maaniitty T, Stenström I, Bax JJ, Uusitalo V, Ukkonen H, Kajander S *et al.* Prognostic value of coronary CT angiography with selective PET perfusion imaging in coronary artery disease. *JACC Cardiovasc Imaging* 2017;**10**:1361–70.
11. Stenström I, Maaniitty T, Uusitalo V, Ukkonen H, Kajander S, Mäki M *et al.* Absolute stress myocardial blood flow after coronary CT angiography guides referral to invasive angiography. *JACC Cardiovasc Imaging* 2019;**12**:2266–7.
12. Harjulahti E, Maaniitty T, Nammas W, Stenström I, Biancari F, Bax JJ *et al.* Global and segmental absolute stress myocardial blood flow in prediction of cardiac events: [^{15}O] water positron emission tomography study. *Eur J Nucl Med Mol Imaging* 2021;**48**:1434–44.
13. Benjamins JW, Yeung MW, Maaniitty T, Saraste A, Klén R, van der Harst P *et al.* Improving patient identification for advanced cardiac imaging through machine learning—integration of clinical and coronary CT angiography data. *Int J Cardiol* 2021;**335**:130–6.
14. Kajander S, Joutsiniemi E, Saraste M, Pietilä M, Ukkonen H, Saraste A *et al.* Cardiac positron emission tomography/computed tomography imaging accurately detects anatomically and functionally significant coronary artery disease. *Circulation* 2010;**122**:603–13.
15. Danad I, Uusitalo V, Kero T, Saraste A, Raijmakers PG, Lammertsma AA *et al.* Quantitative assessment of myocardial perfusion in the detection of significant coronary artery disease: cutoff values and diagnostic accuracy of quantitative [(15)O]H2O PET imaging. *J Am Coll Cardiol* 2014;**64**:1464–75.
16. Joutsiniemi E, Saraste A, Pietilä M, Mäki M, Kajander S, Ukkonen H *et al.* Absolute flow or myocardial flow reserve for the detection of significant coronary artery disease? *Eur Heart J Cardiovasc Imaging* 2014;**15**:659–65.
17. Santosa F, Symes W. Linear inversion of band-limited reflection seismograms. *SIAM J Sci Stat Comput* 1986;**7**:1307–30.
18. Cortes C, Vapnik V. Support-vector networks. *Mach Learn* 1995;**20**:273–97.
19. Vovk V. Kernel ridge regression. In: Schölkopf B, Luo Z, Vovk V, eds, *Empirical Inference: Festschrift in Honor of Vladimir N. Vapnik*. Berlin, Heidelberg: Springer; 2013. p105–16.
20. Zou H, Hastie T. Regularization and variable selection via the elastic net. *J R Stat Soc Ser B (Stat Methodol)* 2005;**67**:301–20.
21. Cox DR. The regression analysis of binary sequences. *J R Stat Soc Ser B (Methodol)* 1958;**20**:215–32.
22. Ho TK. Random decision forests. In: *Proceedings of 3rd International Conference on Document Analysis and Recognition*, Vol. 1, 1995, p278–82.
23. Chen T, Guestrin C. XGBoost: a scalable tree boosting system. In: *The 22nd ACM SIGKDD International Conference*, 2016, p785–94.
24. Pazhenkottil AP, Benz DC, Gräni C, Madsen MA, Mikulicic F, von Felten E *et al.* Hybrid SPECT perfusion imaging and coronary CT angiography: long-term prognostic value for cardiovascular outcomes. *Radiology* 2018;**288**:694–702.
25. Pazhenkottil AP, Nkoulou RN, Ghadri JR, Herzog BA, Buechel RR, Küest SM *et al.* Prognostic value of cardiac hybrid imaging integrating single-photon emission computed tomography with coronary computed tomography angiography. *Eur Heart J* 2011;**32**:1465–71.
26. Taqueti VR, Hachamovitch R, Murthy VL, Naya M, Foster CR, Hainer J *et al.* Global coronary flow reserve is associated with adverse cardiovascular events independently of luminal angiographic severity and modifies the effect of early revascularization. *Circulation* 2015;**131**:19–27.
27. Gould KL, Kitkungvan D, Johnson NP, Nguyen T, Kirkeeide R, Bui L *et al.* Mortality prediction by quantitative PET perfusion expressed as coronary flow capacity with and without revascularization. *JACC Cardiovasc Imaging* 2021;**14**:1020–34.
28. Patel KK, Spertus JA, Chan PS, Sperry BW, Al Badarin F, Kennedy KF *et al.* Myocardial blood flow reserve assessed by positron emission tomography myocardial perfusion imaging identifies patients with a survival benefit from early revascularization. *Eur Heart J* 2020;**41**:759–68.
29. Kumar A, Patel DR, Harb SC, Greenberg NL, Bhargava A, Menon V *et al.* Implementation of a myocardial perfusion imaging risk algorithm to inform appropriate downstream invasive testing and treatment. *Circ Cardiovasc Imaging* 2021;**14**:e011984.
30. Knuuti J, Wijns W, Saraste A, Capodanno D, Barbato E, Funck-Brentano C *et al.* 2019 ESC guidelines for the diagnosis and management of chronic coronary syndromes. *Eur Heart J* 2020;**41**:407–77.
31. Knuuti J, Ballo H, Juarez-Orozco LE, Saraste A, Kolh P, Saskia Rutjes AW *et al.* The performance of non-invasive tests to rule-in and rule-out significant coronary artery stenosis in patients with stable angina: a meta-analysis focused on post-test disease probability. *Eur Heart J* 2018;**39**:3322–30.
32. Leipsic J, Abbara S, Achenbach S, Cury R, Earls JP, Mancini GJ *et al.* SCCT guidelines for the interpretation and reporting of coronary CT angiography: a report of the Society of Cardiovascular Computed Tomography Guidelines Committee. *J Cardiovasc Comput Tomogr* 2014;**8**:342–58.